

# Oligomeric Structure, Dynamics, and Orientation of Membrane Proteins from Solid-State NMR

## Review

Mei Hong<sup>1,\*</sup>

<sup>1</sup>Department of Chemistry  
Iowa State University  
Ames, Iowa 50011

**Solid-state NMR is a versatile and powerful tool for determining the dynamic structure of membrane proteins at atomic resolution. I review the recent progress in determining the orientation, the internal and global protein dynamics, the oligomeric structure, and the ligand-bound structure of membrane proteins with both  $\alpha$ -helical and  $\beta$  sheet conformations. Examples are given that illustrate the insights into protein function that can be gained from the NMR structural information.**

Solid-state NMR (SSNMR) spectroscopy is rapidly maturing as a useful method for determining the atomic-resolution structure of insoluble proteins such as membrane proteins in their natural biological environments. In addition to the static three-dimensional structure, the dynamics, the orientation relative to the membrane, and the oligomeric assembly of these membrane proteins are also actively studied via SSNMR methods. Here, we review the latest progress in SSNMR studies of (1) the oligomeric structure of membrane proteins, i.e., how proteins self-assemble into functional units in the membrane; (2) both the global and internal side chain motion of membrane proteins; (3) the membrane protein orientation; and (4) the location and depth of insertion of membrane proteins. These emphases complement a number of recent reviews on protein structure determination by SSNMR (Baldus, 2006; Bechinger et al., 2004; Bockmann, 2006; Huster, 2005; McDermott, 2004; Opella and Marassi, 2004; Prosser et al., 2006).

### Orientation of Membrane Peptides and Proteins

The principal method that has been used to determine membrane protein orientation is the <sup>15</sup>N-based two-dimensional experiment, PISEMA, in which the N-H dipolar coupling and <sup>15</sup>N chemical shift anisotropy (CSA) of a macroscopically aligned membrane protein are correlated. This method is most suitable for  $\alpha$ -helical proteins, since the <sup>15</sup>N interactions are approximately parallel to the helical axis. However, a number of alternative spin interactions have also been developed and applied to extract membrane protein orientation. These methods allow for the study of both  $\alpha$ -helical and  $\beta$  sheet proteins, and they can determine membrane protein orientational change due to varying conditions such as changes in protein concentration.

#### *Two-Dimensional N-H Dipolar and <sup>15</sup>N Chemical Shift Correlation: Global Helix Orientation*

Two-dimensional N-H dipolar and <sup>15</sup>N correlation spectra of uniformly and selectively <sup>15</sup>N-labeled proteins continue to yield new or refined orientation information

on a number of membrane peptides and proteins, including the transmembrane (TM) domain of the virus protein “u” (Vpu) from HIV-1 (Park et al., 2003), the membrane-bound state of the fd coat protein (Marassi and Opella, 2003), the M2 ion channel proteins of the influenza A virus (Wang et al., 2001) and of the acetylcholine receptor (Opella et al., 1999), bacteriorhodopsin (Kamihira et al., 2005), and a GPCR protein, CXCR1 (Park et al., 2006b). As an example of the information content from this type of experiment, the 50 residue fd coat protein in the membrane was found to contain a surface-bound helix (residues 8–18) connected by a short loop (residues 19–20) to a TM helix (residues 21–45). When the protein is assembled into bacteriophage particles, the surface helix and the TM helix merge into one nearly ideal, straight helix. Moreover, the TM helix of the membrane-bound protein has a distinct kink at residues 38–40, changing the helix tilt angle from 26° to 16° (Marassi and Opella, 2003). This same kink is also present in the phage-bound protein.

The TM domain of the HIV-1 Vpu protein was used to refine PISEMA analysis as well as to extract biophysical principles. When the N-H dipolar couplings are plotted with the residue number, a periodic “dipolar wave” is obtained that exhibits changes in the helix orientation more clearly than the PISEMA spectra themselves (Mascioni and Veglia, 2003; Mesleh et al., 2003). With this analysis, it was found that Vpu has a kink in the middle of the TM domain, causing the tilt angle to change by ~3° in the DOPC/DOPG membrane (Park et al., 2003). When incorporated into membranes of different thicknesses, Vpu changes its tilt angle to minimize the hydrophobic mismatch. The average helix tilt angles are 18°, 27°, 35°, and 51°, respectively, in lipid membranes with 18:1, 14:0, 12:0, and 10:0 acyl chains (Park and Opella, 2005). Interestingly, the kink disappears in the thinner membranes with 14-carbon to 10-carbon chains.

The macroscopic alignment techniques include both mechanical alignment on glass plates, usually with the alignment axis parallel to the magnetic field ( $B_0$ ), and magnetic alignment with bicelles, with the alignment axis perpendicular or parallel to  $B_0$ . In the case of perpendicular bicelles, although the alignment axis is not along  $B_0$ , orientationally resolved spectra are still obtained since the bicelle-protein complex normally undergoes fast uniaxial rotation diffusion around the bicelle axis (Tian et al., 1998). The bicelle approach was recently shown to give better-resolved spectra than glass plate samples (Figure 1) (De Angelis et al., 2004). Interestingly, the structure of the bicelle is still under debate: discs, perforated sheets, and elongated cylindrical micelles have been proposed (Gaemers and Bax, 2001; Harroun et al., 2005; van Dam et al., 2004, 2006).

Recently, an alternative substrate-supported alignment technique that involves nanoporous anodic aluminum oxide (AAO) disks was developed (Chekmenev et al., 2005; Lorigan et al., 2004). When the AAO surface is perpendicular to  $B_0$ , the lipid bilayer normal inside the nanotubes is also perpendicular to  $B_0$ . These AAO membranes have better thermal conductivity, and they allow

\*Correspondence: mhong@iastate.edu

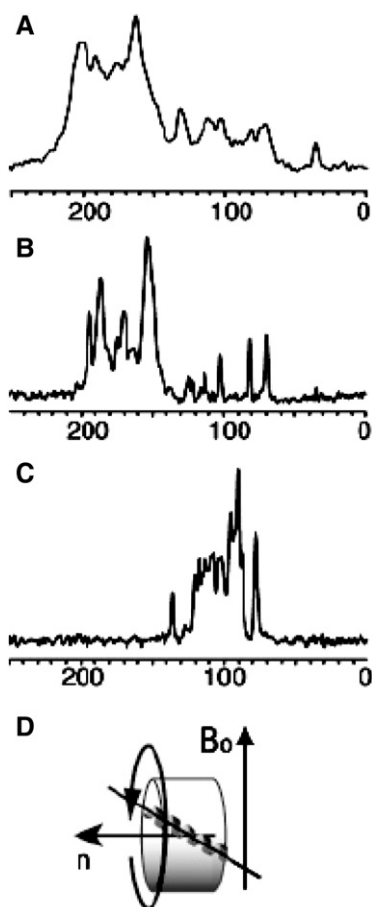


Figure 1.  $^{15}\text{N}$  Chemical Shift Spectra of the Uniformly  $^{15}\text{N}$ -Labeled Vpu TM Domain under Different Alignment Conditions

(A–C) The protein is in (A) a glass plate sample with the alignment axis parallel to  $B_0$ , in (B) flipped bicelles, in which the alignment axis is parallel to  $B_0$ , and in (C) unflipped bicelles, in which the alignment axis is perpendicular to  $B_0$ .

(D) Diagram of an unflipped bicelle containing a TM helix (reproduced from De Angelis et al., 2004 with permission).

the external environment, such as pH and ion concentration, to be readily adjusted in membrane protein structural studies.

#### $^{19}\text{F}$ Chemical Shift Anisotropy:

##### Concentration-Dependent Orientation

Ulrich and coworkers have developed a novel  $^{19}\text{F}$  NMR strategy to determine membrane protein orientations. The approach uses the F–F dipolar coupling in  $\text{CF}_3$ -Phg to determine membrane peptide orientation. The magnitude of the coupling is obtained from the splitting, while the sign of the dipolar coupling is obtained from the anisotropic chemical shift (Glaser et al., 2004). The advantages of  $^{19}\text{F}$  as an orientational probe include its large CSA and strong  $^{19}\text{F}$ - $^{19}\text{F}$  dipolar coupling, which give high angular resolution, its high sensitivity due to the large gyromagnetic ratio, and the lack of background signals in membrane proteins. The  $^{19}\text{F}$  spin needs to be incorporated into the protein chemically. The fluorinated residues that have been demonstrated so far include 4- $^{19}\text{F}$ -phenylglycine (Phg) (Afonin et al., 2003),  $\text{CF}_3$ -Phg (Glaser et al., 2004),  $\text{CF}_3$ -Ala (Grage and Ulrich, 2000), and 4- $^{19}\text{F}$ -Phe (Buffy et al., 2005).

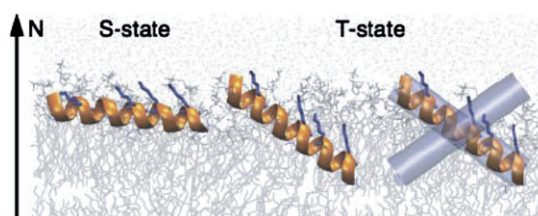


Figure 2. The Orientation of the PGLa Helix from the  $^{19}\text{F}$  Chemical Shift and Dipolar Coupling Constraints

As P/L increases from the left to the right, the helix orientation changes from in-plane ( $\tau = 89^\circ$ ) to an obliquely tilted and inserted state ( $\tau = 123^\circ$ ). The inserted state was hypothesized to be dimerized (reproduced from Glaser et al., 2005 with permission).

Using glass-plate-aligned samples and  $^{19}\text{F}$  CSA and F–F dipolar coupling measurements, Ulrich and coworkers investigated the orientation and orientational changes of the  $\alpha$ -helical antimicrobial peptide PGLa (Glaser et al., 2004, 2005), the cyclic  $\beta$  sheet antimicrobial peptide gramicidin S (Salgado et al., 2001), and a fusogenic peptide, B18 (Afonin et al., 2004). The magainin-analog PGLa exhibits an in-plane orientation at low P/L molar ratios (1:200), but this changes to an oblique orientation, with the helical axis at an angle of  $123^\circ$  with the bilayer normal, when the P/L ratio increases to 1:50 and higher (Figure 2). At intermediate concentrations, the peptide undergoes fast exchange between these two orientations (Glaser et al., 2004, 2005). The tilt angle does not have the typical double degeneracy between  $\tau$  and  $180 - \tau$ , because the  $^{19}\text{F}$  chemical shift spectra are modulated by the F–F dipolar coupling within the  $\text{CF}_3$  group of the  $\text{CF}_3$ -Phg labels, thus yielding the sign of the dipolar coupling. The rotation angle of both orientations is consistent with the amphipathic character of the peptide, putting the hydrophilic side chains toward the membrane surface. In applying this  $^{19}\text{F}$  NMR technique, it is important to check that the biological function of the peptide is not adversely affected by the replacement of the natural residues with  $\text{CF}_3$ -Phg or 4F-Phg. The high sensitivity of  $^{19}\text{F}$  NMR spectra allows for the study of membrane peptide orientation over a wide P/L range, thus directly testing the hypothesis of orientational change.

#### $^2\text{H}$ Quadrupolar Coupling of Ala Methyl Groups:

##### Another Orientational Probe

Methyl-deuterated Ala is a simple and robust orientational probe. The three-site jump of the Ala methyl group occurs around the  $\text{C}\alpha$ - $\text{C}\beta$  axis; thus, the quadrupolar splitting reflects the orientation of the  $\text{C}\alpha$ - $\text{C}\beta$  bond relative to the alignment axis without other complicating torsional motion of the side chain. Combined with  $^{15}\text{N}$  chemical shift constraints, the  $^2\text{H}$  probe has been used to determine the orientation of designed amphipathic peptides KL14 and KL26 and a hydrophobic peptide, h $\Phi$ 19W (Aisenbrey and Bechinger, 2004b). The KL peptides were found to be parallel to the membrane plane with a rotation angle that places the polar residues toward water and the hydrophobic residues toward the membrane, while h $\Phi$ 19W was found to be a TM peptide. Since  $^2\text{H}$  NMR has comparable or higher sensitivity than  $^{15}\text{N}$  NMR, and since the acquisition of quadrupolar spectra can be much faster than  $^{15}\text{N}$  spectra due to the absence of  $^1\text{H}$  decoupling, this Ala- $^2\text{H}$  NMR is an

appealing approach for orientation determination. However, a single-site  $^2\text{H}$  coupling is usually insufficient to obtain a unique solution to both the tilt and rotation angles of the peptide, similar to the degeneracy that would be present in 1D  $^{15}\text{N}$  spectra of singly labeled peptides (hence the need for multiple  $^{15}\text{N}$  labeling and two-dimensional PISEMA spectra). Thus, systematic site-specific deuteration and Ala mutation have recently been reported to restrain the global orientation of membrane peptides (Strandberg et al., 2006).

#### $^{13}\text{C}$ CO Chemical Shift Anisotropy:

##### $\beta$ Sheet Membrane Proteins

The  $^{13}\text{C}$  CO chemical shift tensor is a useful probe of  $\beta$  sheet peptide orientation, because the  $\sigma_{xx}$  principal axis is aligned along the strand axis, while the  $\sigma_{zz}$  axis is perpendicular to the  $\beta$  sheet plane. Therefore, for a uniaxially aligned peptide with the bilayer normal parallel to the magnetic field, the observation of a frequency close to 245 ppm ( $\sigma_{xx}$ ) indicates that the strand axis is parallel to the bilayer normal (a TM peptide, for example), while a peak close to 95 ppm ( $\sigma_{zz}$ ) indicates that the  $\beta$  sheet plane normal is parallel to the bilayer normal (for example, an in-plane peptide).  $^{13}\text{C}$  CO chemical shift constraints have been used to determine the orientation of PG-1 (Yamaguchi et al., 2002) and TP-I (Hong and Doherty, 2006), two disulfide-stabilized  $\beta$  sheet antimicrobial peptides. PG-1 was found to exhibit an oblique orientation, with the strand axis tilted by  $\sim 55^\circ$  from the normal of the DLPC membrane. TP-I, on the other hand, is much more parallel to the membrane plane, with the strand axis tilted by only  $\sim 20^\circ$  from the plane. This difference is consistent with the different insertion depths of the two peptides: PG-1 is well inserted into the hydrophobic center of the membrane (Buffy et al., 2003a), while TP-I lies at the glycerol backbone region, in contact with the top of the acyl chains, but not the membrane center (Doherty et al., 2006). These differences are attributed to the different amphipathic structures of the two peptides. PG-1 has a hydrophilic-hydrophobic separation along the strand axis; thus, the hydrophobic domain can insert in a TM fashion. TP-I, on the other hand, exhibits side chain amphipathicity below and above the  $\beta$  hairpin plane, but no backbone amphiphilicity, thus favoring an in-plane orientation.

#### Membrane Protein Dynamics

##### Rigid-Body Uniaxial Rotational Diffusion

Rigid-body uniaxial rotational diffusion of membrane peptides and proteins has recently become a topic of interest due to its relevance for orientation determination and for understanding the complete physical state of the protein. As a result of the fluidity of the liquid-crystalline lipid bilayer, membrane proteins undergo Brownian motions in the two-dimensional membrane at rates given by the Saffman-Delbrück equation (Saffman and Delbrück, 1975):

$$D_r = \frac{kT}{4\pi\eta r^2 h}, \quad (1)$$

where  $\eta$  is the viscosity of the membrane,  $T$  is the absolute temperature, and  $r$  and  $h$  are the radius and height, respectively, of the diffusing cylinder in the membrane. This equation predicts that TM proteins with radii up to

$\sim 12 \text{ \AA}$  should undergo uniaxial rotations that are fast compared to the  $^2\text{H}$  quadrupolar couplings of  $\sim 125 \text{ kHz}$  and thus should average the  $^2\text{H}$  NMR spectra. If  $^{15}\text{N}$  and  $^{13}\text{C}$  chemical shift interactions at magnetic field strengths of 9.4–14.1 Tesla are used to monitor motion, then these smaller interactions (up to  $\sim 6 \text{ kHz}$ ) allow proteins with radii up to  $\sim 40 \text{ \AA}$  to still remain in the fast motional limit. Thus, motionally averaged  $^{15}\text{N}$  and  $^{13}\text{C}$  chemical shift spectra are expected even for relatively large membrane proteins.

Many experimental reports of such uniaxial rotational diffusion have been given. These include ion channel peptides such as gramicidin A (Ketchum et al., 1993), designed synthetic peptides such as KL14 and h $\Phi$ 19W (Aisenbrey and Bechinger, 2004a), antimicrobial peptides such as PG-1 and ovispirin (Yamaguchi et al., 2001, 2002), and helical bundles such as the TM domain of the M2 protein of influenza A virus (Song et al., 2000). These peptides can have both  $\alpha$ -helical and  $\beta$  sheet conformation, and they can be either TM or parallel to the membrane plane. Therefore, rotational diffusion appears to be universal given a suitable size and viscosity of the membrane. In all cases reported, the uniaxial rotational diffusion is around the bilayer normal, which is the unique direction in the two-dimensional membrane.

Using  $^2\text{H}$  quadrupolar couplings, C-H and N-H dipolar interactions,  $^{13}\text{C}$  and  $^{15}\text{N}$  chemical shift anisotropies, and  $^1\text{H}$  relaxation time measurements, Hong and coworkers characterized the rates and amplitude of the uniaxial rotational diffusion of the M2 TM peptide (M2TMP) of influenza A virus (Cady and Hong, 2006). They found that the rotational diffusion depends on the sample preparation condition: mixing of peptide and lipid in organic solvents prior to the self-assembly of lipid bilayers promotes rotational diffusion, while direct mixing of the peptide with the lipid vesicle solution produces proteins without fast global rotation on the  $^2\text{H}$  NMR timescale. These suggest preferential aggregation of the peptide when bound to lipid vesicle solutions.

As expected from Equation 1, membrane protein orientation affects the rotational diffusion time constants due to the quadratic dependence on  $r$  and the linear dependence on  $h$ . A surface-bound membrane peptide has a much larger radius than the same-sized protein in a TM orientation and thus should be less mobile. Indeed, KL26, a 26 residue amphipathic, in-plane helical peptide consisting of Lys and Leu residues, was shown by  $^{15}\text{N}$  chemical shift spectra and  $^2\text{H}$  NMR spectra to be immobilized on these timescales (Aisenbrey and Bechinger, 2004b). The radius of the peptide is  $\sim 39 \text{ \AA}$ . In comparison, the 25 residue M2TMP with a similar length rotates even in the tetrameric state because of its smaller  $r$  for diffusion (Song et al., 2000). The same KL peptide with only 14 residues (KL14), which also has an in-plane orientation, does undergo fast uniaxial rotational diffusion on the  $^{15}\text{N}$  CSA and  $^2\text{H}$  timescales. Thus, the upper size limit of surface-bound peptides for rotational diffusion lies between 21  $\text{ \AA}$  and 39  $\text{ \AA}$ .

When membrane proteins are bound to lipid bicelles in solution (Prosser et al., 1998; Sanders et al., 1994), uniaxial rotational diffusion around the bicelle normal occurs as a result of the combined motion of the bicelle in solution and the possible rotational diffusion of the protein in the bicelle. Although the exact nature of the

motion has not been investigated, this motion has been utilized to good effect to determine orientational constraints (Figure 1) (De Angelis et al., 2004; Park et al., 2006a).

The rotational diffusion rates of membrane proteins are influenced by the membrane thickness (through  $h$ ) and by temperature. Below the phase transition temperature the motion ceases. Increasing the membrane thickness also slows down the motion more rapidly. Examples of these phenomena are reported for the KL peptides (Aisenbrey and Bechinger, 2004a) and the M2TMP of influenza A virus (Cady and Hong, 2006).

#### **Functional Dynamics of Membrane Proteins**

Posttranslational lipid modifications are a common motif of membrane proteins. The role of the covalently bound lipid chains in membrane protein function was investigated for the human N-ras protein, a signal transduction protein involved in cancer formation. Huster and coworkers measured the  $^2\text{H}$  quadrupolar couplings and spin-lattice relaxation rates ( $R_{1\rho}$ ) to compare the dynamics of the DMPC matrix and the two thioether-linked lipid chains of the ras peptide. They found that the ras lipid chains exhibit much larger amplitudes and higher rates of motion than the DMPC matrix (Vogel et al., 2005). This enhanced mobility may facilitate the insertion of the peptide into the lipid-water interface of the membrane (Huster et al., 2003). In fact, since the peptide backbone is conformationally disordered, membrane binding of the ras peptide appears to be driven mainly by the favorable energy associated with lipid chain insertion (Huster et al., 2003).

The rotational motion of membrane peptides may be inhibited when the aggregation state of the protein or the modes of protein-lipid interaction change. For example, the antimicrobial peptide PG-1 undergoes fast uniaxial rotational diffusion in DLPC bilayers (12:0 chains), but it becomes immobilized in POPC and POPE/POPG bilayers (16:0 and 18:1 chains) (Buffly et al., 2003b). Since PG-1 selectively targets bacterial membranes rich in anionic lipids (POPG) and long palmitoyl (16:0) and oleoyl (18:1) chains, the immobilization in the POPx lipids suggests immobilization as part of the mechanism of action of PG-1.

#### **Side Chain Methyl Dynamics Probes Membrane Protein Interfaces**

Smith and coworkers have used  $^2\text{H}$  MAS spectra of methyl-deuterated Leu and Val to probe the packing of membrane protein interfaces. Unlike Ala methyl groups, Leu and Val methyl groups are several aliphatic groups away from the backbone; thus, they can undergo torsional motions around  $\text{C}\alpha\text{-C}\beta$  (for Val) and  $\text{C}\beta\text{-C}\gamma$  bonds (for Leu) if these side chains are not restricted by tight packing with another peptide or with another side chain in the same peptide.

An interesting example of intrahelical conformational restriction is seen in the TM domain of glycoporphin A (GpA) (Liu et al., 2003). Two Val residues, V80 and V84, showed spectra indicative of only methyl three-site jumps but no rotation around the  $\text{C}\alpha\text{-C}\beta$  bond. This is true for both the dimer and monomer states of the peptide, the latter obtained from a site-specific mutation that disrupts dimerization. Thus, V80 and V84 are immobilized by intrahelical contacts already present in the monomer state. The implication is that dimerization

does not involve the loss of side chain entropy. In contrast, V82 exhibits slightly reduced  $^2\text{H}$  quadrupolar coupling (95% that of V80 and V84). Because residue  $i$  in a helix experiences intrahelical contacts with the side chain of  $i+4$ , V80 (with V84) and V84 (with V88) were constrained by their  $\beta$ -branched  $i+4$  neighbors, while V82, with an  $i+4$  neighbor of G86, has reduced packing constraints.

This methyl  $^2\text{H}$  NMR dynamics approach was used to probe the interfacial structures of the TM domain of a viral glycoprotein, gp55-P (Liu et al., 2005), and a designed peptide, GCN4-MS1, that forms homo-oligomeric helical bundles in the membrane (Howard et al., 2005). The general approach is to methyl-deuterate several consecutive Leu (or Val) residues, thus covering different rotation angles around the helix axis and sampling their mobility. In the dimeric gp55-P, the  $^2\text{H}$  MAS sideband spectra of four consecutive Leus identified L399 to be the most immobile group, without  $\text{C}\alpha\text{-C}\beta$  and  $\text{C}\beta\text{-C}\gamma$  torsional motion, thus placing it at the dimer interface. Further, by measuring the  $^2\text{H}$  spectra of 2 residues upstream and downstream of the Leu stretch, the helical crossing angle was determined to be right handed. Thus,  $^2\text{H}$  NMR dynamics measurements give insights into the oligomeric interface of the peptide. Similarly, when 3 Leu residues, 8–10, in GCN4-MS1 were deuterated, the  $^2\text{H}$  sideband spectra show smaller couplings of 14 kHz for L8 and L9, but 18 kHz for L10, indicating that the latter lies in the peptide-peptide interface, while L8 and L9 face the lipids (Figure 3). These provide experimental support for the trimeric, left-handed coiled-coil structure model for this peptide.

#### **Membrane Protein Oligomeric Structure**

Oligomerization is a common phenomenon among ion channels, fusion proteins, and membrane-disruptive proteins. The oligomeric state, i.e., the number of peptides forming a well-defined structural and functional unit that shares common dynamic properties, has been rarely determined. The oligomeric structure, in terms of the mutual orientation and packing of the peptide chains, is also less studied than the monomeric structure. For membrane-disruptive peptides, it is often unclear whether the immobilized proteins form structured or unstructured aggregates in the membrane. However, emerging techniques and recent reports have shown that membrane peptides can form structured aggregates with well-defined distances within 10–15 Å.

#### **Oligomeric Structure of Membrane-Disruptive Peptides**

Schaefer and coworkers used multinuclear REDOR experiments to determine the aggregation state and lipid contact of a peptide antibiotic, K3 (Toke et al., 2004b). K3 is a synthetic analog of PGLa, which is a magainin-like  $\alpha$ -helical peptide found in the skin secretions of *Xenopus laevis*. In a mixture of  $^{13}\text{C}$ -labeled and  $^{19}\text{F}$ -labeled peptides, they found significant intermolecular  $^{13}\text{C}$ - $^{19}\text{F}$  dipolar couplings. From the plateau of the REDOR dephasing, the fraction of the aggregated peptide chains was estimated to be 50%–80% at a L/P ratio of 20 and decreases with decreasing peptide concentration. The interhelical distances were 4.5–10.5 Å, depending on the label positions, and constrain the helices to be parallel to each other. Differential REDOR dephasing was

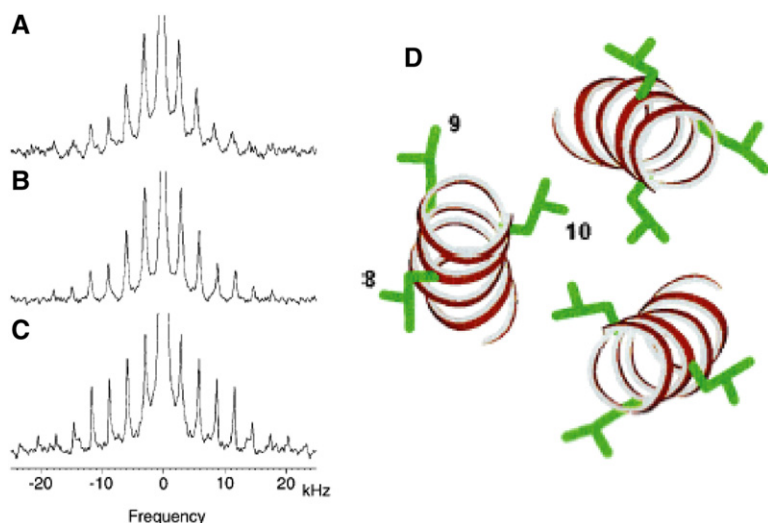


Figure 3.  $^2\text{H}$  Quadrupolar Couplings for the Identification of the Oligomeric Interface in a GCN4-MS1 Variant

(A–C) Spectra of methyl-deuterated (A) L8, (B) L9, and (C) L10 in DMPC-bound peptide. (D) Model of GCN4-MS1. The dynamically restricted L10 lies in the bundle interior, while L8 and L9 face the lipids (reproduced from Howard et al., 2005 with permission).

observed for different  $^{13}\text{C}$ O chemical shift sidebands, indicating that the intermolecular C-F vector has a well-defined orientation with respect to the  $^{13}\text{C}$ O chemical shift tensor. This suggests that the K3 aggregate is probably not larger than a dimer, as orientational specificity would be lost in a larger aggregate. With this dimer approximation, an interhelical crossing angle of  $\sim 20^\circ$  was estimated.

The same strategy of measuring intermolecular distances to determine the oligomeric structure was also employed by Hong and coworkers to study a  $\beta$  hairpin antimicrobial peptide, PG-1 (Mani et al., 2006b). There, long-range  $^{13}\text{C}$ - $^{19}\text{F}$  distances ( $\sim 10$  Å) are augmented by a short intermolecular  $^{13}\text{C}$ - $^1\text{H}$  distance ( $\sim 2.5$  Å) determined by an  $^{15}\text{N}$ -detected  $^{13}\text{C}$ - $^1\text{H}$  REDOR experiment. The high gyromagnetic ratio of  $^1\text{H}$  enables the measurement of distances that are too long to be detectable by  $^{13}\text{C}$ - $^{15}\text{N}$  dipolar couplings (Schmidt-Rohr and Hong, 2003). These distance constraints indicate that the  $\beta$  hairpins are aligned parallel to each other, with the C-terminal strand lining the dimer interface. The short CO- $\text{H}^{\text{N}}$  distance suggests that dimerization is mediated by intermolecular hydrogen bonds between the C=O and H-N groups of opposing strands. The resulting dimer is highly amphipathic (Figure 4), which may facilitate peptide insertion into the amphipathic membrane.

#### Oligomeric Structure of Fusion Peptides

The conformation and oligomerization of several fusion peptides have been studied. One fusion peptide is the B18 peptide (residues 103–120) of the sea urchin fertilization protein bindin, which mediates fusion between sperm and egg cells. Binding of B18 to  $\text{Zn}^{2+}$  through a His-rich motif enhances the fusion activity of the peptide in zwitterionic membranes. In aqueous solution, the peptide is unstructured in the absence of  $\text{Zn}^{2+}$  and  $\alpha$ -helical after  $\text{Zn}^{2+}$  binding (Ulrich et al., 1998). Binding to DPC or SDS micelles changes the peptide conformation to  $\alpha$ -helical (Glaser et al., 1999). In lipid membranes, SSNMR and FT-IR data indicate that the  $\text{Zn}^{2+}$ -bound B18 adopts a parallel  $\beta$  sheet structure at high concentrations (P/L = 1:12), but that it is  $\alpha$ -helical at low concentrations (P/L = 1:50) (Barre et al., 2003). This parallel  $\beta$  sheet conformation is seen from both  $^{13}\text{C}$  chemical

shifts and  $\phi$  torsion angles of specific residues. Further,  $^2\text{H}$  order parameters of lipid chains decrease significantly upon B18 binding, indicating that B18 penetrates the membrane (although to what extent is not known). Since it is energetically unfavorable for non-hydrogen-bonded polar backbone groups (N-H, C=O) to insert into the membrane, the  $^2\text{H}$  data and the peptide conformation imply that the B18  $\beta$  strand is probably oligomerized. This is consistent with the rigidity of the B18 backbone evidenced from dipolar couplings.

The oligomeric structure of the 23 residue N-terminal fragment of the HIV-1 gp41 envelope protein, which fuses the membranes of HIV-1 virus and the target cells, was also studied by SSNMR. Sideband intensities in slow-spinning two-dimensional  $^{13}\text{C}$  exchange spectra indicate that the fusion peptide adopts  $\beta$  sheet conformation in lipid membranes mimicking the composition of the HIV-1 virus and its target T cells (Yang et al., 2001). Intermolecular  $^{13}\text{C}$ - $^{15}\text{N}$  distance measurements of site-specifically labeled peptides indicate that the peptides form intermolecular  $\beta$  sheets with roughly equal populations of the parallel and antiparallel orientations (Yang and Weliky, 2003). Finally, mutants of the peptide that are monomeric in solution were found to

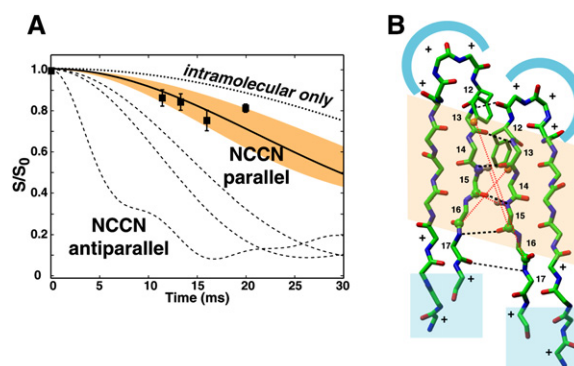


Figure 4. Dimer Structure of PG-1 in POPC Membranes

(A and B) (A)  $^{13}\text{C}$ - $^{19}\text{F}$  REDOR distance data. (B) Dimer model of PG-1 based on distance restraints. The  $\beta$  hairpin molecules form parallel dimers with the C-terminal strand lining the dimer interface (reproduced from Mani et al., 2006b with permission).

adopt a similar  $\beta$  sheet conformation as peptides that are oligomeric in solution (Yang et al., 2004). These findings suggest that membrane binding converts the monomeric fusion peptides into oligomeric  $\beta$  sheets. Interestingly, the peptide is  $\alpha$ -helical in DPC micelles and in anionic POPC/POPG membranes, and both the  $\alpha$ -helical and  $\beta$  sheet forms can be fusogenic. These findings underscore the importance of membrane composition in regulating membrane peptide structure.

#### Oligomeric Structures of TM Helical Bundles

The oligomeric structure of several TM helical proteins, including the erythrocyte protein GpA (Smith et al., 2001b), the Neu receptor tyrosine kinase involved in signal transduction (Smith et al., 2002), and the calcium-regulating protein phospholamban (Smith et al., 2001a), have been investigated by Smith and coworkers. The studies primarily used homonuclear (e.g.,  $^{13}\text{C}$ - $^{13}\text{C}$ ) and heteronuclear (e.g.,  $^{13}\text{C}$ - $^{15}\text{N}$ ) distances between carefully selected residues to probe the principles of protein folding such as helix dimerization motifs, interhelical hydrogen bonding, and the contribution of side chain entropy to the free energy of oligomerization. In GpA, distance experiments revealed several short interhelical contacts (4.0 Å–4.8 Å) involving two key Gly residues, G79 and G83 (Smith et al., 2001b), which provide direct evidence for the essential role of small Gly residues in stabilizing interhelical interfaces. This Gly surface enables the tight packing of several  $\beta$ -branched residues (I78, V80, and V84) across the dimer interface (Figure 5).

The packing of the only polar residue, T87, in the GpA-binding motif was also studied. Based on the short interhelical distance of 4.0 Å between the  $\gamma$ - $^{13}\text{C}$  of T87 and I88  $^{15}\text{N}$ , and the  $\chi_1$  torsion angle of T87, it was suggested that the hydroxy group of T87 forms an interhelical hydrogen bond with the V84 carbonyl group.

In the Neu receptor tyrosine kinase, the chemical signal of binding the extracellular domain is relayed to the TM domain by causing its dimerization, which then leads to autophosphorylation of the intracellular domain. Rotational resonance ( $R^2$ )  $^{13}\text{C}$ - $^{13}\text{C}$  distance measurements and REDOR  $^{13}\text{C}$ - $^{15}\text{N}$  distance measurements found specific close interhelical contacts between the backbone carbons of G665 and E664, but no close contacts between the Glu/Gln side chain and the Gly backbone (Smith et al., 2002). These findings indicate that dimerization is not mediated by hydrogen bonding of polar side chains, but by the presence of the small Gly residue.

#### Determination of the Oligomeric Number

While  $R^2$  and REDOR experiments give quantitative intermolecular distances that indicate oligomerization, they do not give the oligomeric number of the membrane protein. The determination of the oligomeric number typically requires either low-resolution techniques such as gel electrophoresis and analytical ultracentrifugation or indirect NMR evidence such as orientation specificity of the NMR peak intensities or the narrowness of the measured distance distribution (Toke et al., 2004b).

Two direct “spin-counting” techniques are in fact available in NMR to determine the aggregation number. One is the multiple-quantum (MQ) technique (Yen and Pines, 1983), which has been successfully used to determine that the  $\beta$  sheet peptide of the Alzheimer’s  $\beta$ -amyloid fibril ( $A\beta$ ) is organized in a parallel fashion (Antzutkin et al., 2000; Antzutkin and Tycko, 1999). The highest

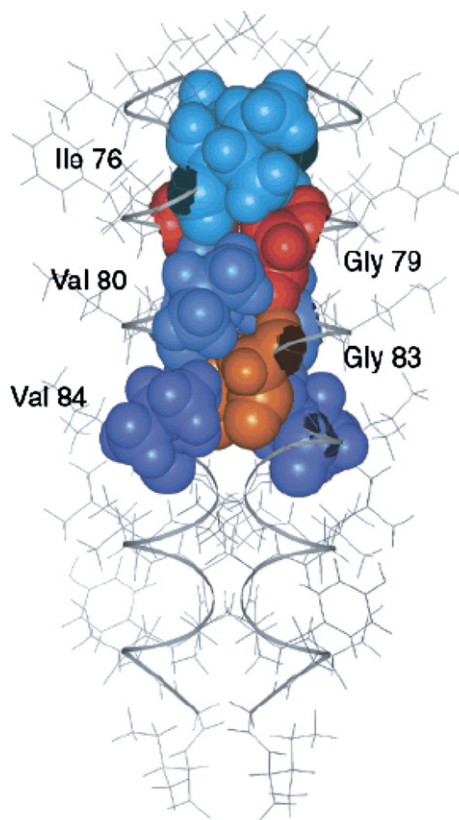


Figure 5. Structural Model of the Glycophorin A TM Dimer from Interhelical  $^{13}\text{C}$ - $^{13}\text{C}$  Distances

The  $\beta$ -branched amino acids I78, V80, and V84 form a ridge that packs against the surface formed by G79 and G83 (reproduced from Smith et al., 2001b with permission).

quantum number observed in site-specifically labeled  $A\beta$  corresponds to the minimum number of molecules in close proximity. This MQ NMR approach can, in principle, be applied to membrane proteins, provided that the sensitivity limitation associated with the static wide-line spectra can be overcome.

The second approach is orientation-dependent spin diffusion, adapted from an exchange NMR technique originally designed for studying slow molecular motions (deAzevedo et al., 1999, 2000). The experiment detects the intensity of a stimulated CSA echo after time was allowed for spin diffusion to occur. Magnetization transfer to spins with different orientations causes CSA changes, which reduces the echo intensity. The equilibrium echo intensity is  $1/N$  for a spin cluster of size  $N$ . Thus, by combining measurement of the equilibrium echo intensity with singly labeling the peptide to ensure that spin diffusion is intermolecular, one can determine the aggregation number of the membrane protein complex. This experiment requires that the dipolar coupling is not too weak for typical intermolecular distances in oligomeric membrane peptides. Thus, the high- $\gamma$  spin  $^{19}\text{F}$  was used to measure spin diffusion, and distances up to  $\sim 15$  Å were shown to be detectable (Buffy et al., 2005).

The  $^{19}\text{F}$  spin diffusion experiment was used to determine the oligomeric number of PG-1 in various membranes. In zwitterionic POPC membranes, a dimer was

detected at high peptide concentrations (P/L = 1:12.5), while mixtures of monomers and dimers were found at P/L = 1:30 (Buffy et al., 2005). In POPE/POPG membranes mimicking the composition of the bacterial inner membrane, spin counting gave a cluster size of two for  $^{19}\text{F}$  labels at the C-terminal strand and the N-terminal strand of the  $\beta$  hairpin (Mani et al., 2006a). These findings suggest that the hairpins form a multimeric  $\beta$  barrel with like-stranded intermolecular interfaces. Thus, multisite labeling is important for determining the global oligomeric state of a membrane protein assembly and for extending the distance range to  $>15$  Å.

Interestingly, the PG-1 aggregate state changes in membranes of different compositions. In cholesterol-containing zwitterionic membranes mimicking the plasma membrane of eukaryotic cells, PG-1 forms larger aggregates of four or more peptides on the surface of the lipid bilayer (Mani et al., 2006a). This contrasts with the  $\beta$  barrel in the anionic membrane, which is found to be TM. The difference in oligomeric state and depth of insertion correlates well with the reduced hemolytic activity and the strong antimicrobial activity of the peptide.

#### **Location of Oligomeric Proteins in the Lipid Membrane**

Often it is insufficient to determine only the oligomeric number and oligomeric structure of membrane proteins without also characterizing their location in the membrane.  $^1\text{H}$  spin diffusion from lipid chains to the protein has become a common tool for obtaining semiquantitative distances of a protein to the membrane hydrophobic center (Huster et al., 2002). More quantitative distances can be obtained from the peptide-lipid headgroup distance (through lipid  $^{31}\text{P}$  spins) or peptide-lipid tail (through fluorinated chain ends) distances (Toke et al., 2004a). Paramagnetic ions also provide an effective distance probe, through distance-dependent relaxation enhancement of the nuclear spins (Buffy et al., 2003a; Prosser et al., 2000; Tuzi et al., 2001).

The lipid contact of the K3 peptide in the DPPC/DPPG membrane was examined in detail by using REDOR distance experiments (Toke et al., 2004a).  $^{13}\text{C}$  and  $^{15}\text{N}$  labels placed in the middle of the helical peptide showed distances from the lipid  $^{31}\text{P}$  of 5–6 Å for ~30% of the peptide. Close peptide contacts with the lipid tail, with  $^{13}\text{C}$ - $^{19}\text{F}$  distances of  $7.7 \pm 3.6$  Å, were also found. Finally, the lipid headgroup-lipid tail  $^{31}\text{P}$ - $^{19}\text{F}$  distances decreased in the presence of K3. These distance constraints rule out the barrel-stave model and the carpet model, but they provide strong support for the toroidal pore model, in which the lipid membrane is distorted by the peptide and the two lipid leaflets merge into one (Figure 6) (Ludtke et al., 1996).

Based on  $^{31}\text{P}$  line shapes (Yamaguchi et al., 2002) and the close contact of PG-1 with the hydrophobic part of the membrane (Mani et al., 2006a), Hong and coworkers also concluded that PG-1 forms toroidal pores in anionic membranes. However, for both K3 and PG-1, the organization and packing of the lipid molecules at the sites of the peptide remain unclear. One of the key questions is how the lipid chains avoid steric conflicts with each other and with peptides in the restricted space of the pores. A partial answer may lie in lipid chain upturns, which have been reported for hydrated membranes even in the absence of membrane proteins (Huster

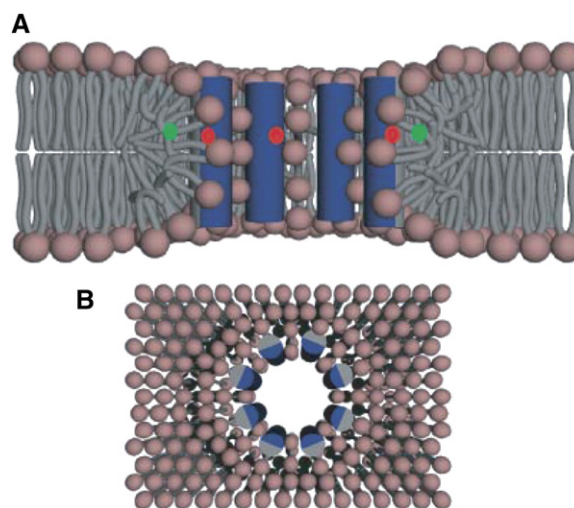


Figure 6. Toroidal Pore Model for the Antimicrobial Peptide K3 (A and B) (A) Side view. (B) Top view. The peptide distance to the lipid headgroup and lipid tail as well as the lipid headgroup-tail distance support this model (reproduced from Toke et al., 2004a with permission).

et al., 1999; Huster and Gawrisch, 1999). Such chain upturns may be an energetically favorable solution to the steric problem of the toroidal pore. The emerging experimental studies suggest that the true structure of these peptide-lipid assemblies may blend features of the barrel-stave model and the toroidal pore model, in that the proteinaceous part of the pore forms well-defined structures, which is a  $\beta$  barrel in the case of PG-1 and a dimeric helical bundle in the case of K3, while the lipidic part of the membrane is orientationally disordered.

#### **High-Resolution Structure of Integral Membrane Proteins and Ligand-Binding Interfaces**

Determination of the complete three-dimensional structure of membrane proteins by SSNMR is still in its infancy. But, significant progress has been made on a few membrane proteins, especially in terms of their ligand-bound structure. These include the outer membrane protein G of *E. coli* (Hiller et al., 2005), the bound structure of neurotensin with its G protein-coupled receptor (GPCR) (Luca et al., 2003), and the binding between a toxin and a chimaeric potassium channel protein (Lange et al., 2006). Neurotensin is a small peptide agonist of a GPCR receptor, NTS-1 (101 kDa). In the high-affinity, bound state, neurotensin conformation could not be determined by solution NMR due to immobilization of the receptor-ligand complex. Two-dimensional  $^{13}\text{C}$  double-quantum (DQ) correlation spectra of uniformly  $^{13}\text{C}$ -labeled neurotensin in the free and bound states showed isotropic shift differences that indicate that the peptide changes from a random coil to a  $\beta$  strand upon receptor binding. DQ spectroscopy was necessary to filter out the signals of the large receptor. The study used microgram quantities of the peptide and a few milligrams of the receptor; thus, it is a tour de force in overcoming the sensitivity limit.

The conformational changes in a chimaeric potassium channel, KcsA-Kv1.3, upon binding of a toxin inhibitor

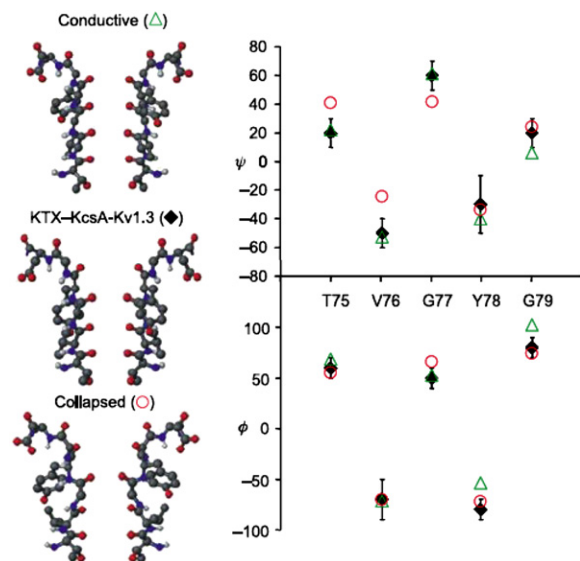


Figure 7. Structures of the Selectivity Filter of the Potassium Channel

Green triangles: high  $K^+$  concentration. Red circles: low  $K^+$  concentration. Black diamond: SSNMR-determined toxin-bound state. The toxin-bound structure is a mix between the two crystal structures. Right: ( $\phi$ ,  $\psi$ ) torsion angles of key residues in the three structures (reproduced from Lange et al., 2006 with permission).

were studied by  $^{13}\text{C}$  chemical shift perturbation analysis and  $^1\text{H}$ - $^1\text{H}$  distance measurement (Lange et al., 2006). By mixing labeled and unlabeled toxin and channel protein, Baldus and coworkers found regions of significant conformational changes in both the toxin and the potassium channel as a result of binding, and their findings revise previous notions of rigid binding sites in the complex. The toxin was proposed to insert more deeply into the selectivity filter than previously thought, and the selectivity filter of the channel was proposed to adopt a novel conformation with features of both the conducting and the collapsed states of the protein (Figure 7). The study highlights the importance of conformational dynamics in membrane protein function.

## Outlook

SSNMR spectroscopy is maturing as a powerful tool for investigating the complex structures of protein-protein assemblies in the membrane, the protein-lipid assembly, and the ligand-bound states of large membrane proteins. Both site-specific distance measurements and uniform  $^{13}\text{C}$  and  $^{15}\text{N}$  labeling that give conformation-dependent or orientation-dependent chemical shifts are viable approaches to membrane protein structure determination. The former requires key residues to be suitably labeled but gives highly accurate structural restraints, while the latter provides cruder but more complete structure information. Membrane protein structure must always be considered in the context of the lipid membrane environment (e.g., the orientation and depth of insertion) and in the context of functional dynamics of the protein. Thus, a comprehensive approach should be employed to truly understand the structure-function relation of these fascinating and important molecules.

## Acknowledgments

This work is partially funded by National Institutes of Health grant GM-066976 and National Science Foundation grant MCB-0543473.

## References

- Afonin, S., Glaser, R.W., Berdichevskaia, M., Wadhvani, P., Guhrs, K.H., Mollmann, U., Perner, A., and Ulrich, A.S. (2003). 4-fluorophenylglycine as a label for  $^{19}\text{F}$  NMR structure analysis of membrane-associated peptides. *ChemBioChem* 4, 1151–1163.
- Afonin, S., Durr, U.H., Glaser, R.W., and Ulrich, A.S. (2004). 'Boomerang'-like insertion of a fusogenic peptide in a lipid membrane revealed by solid-state  $^{19}\text{F}$  NMR. *Magn. Reson. Chem.* 42, 195–203.
- Aisenbrey, C., and Bechinger, B. (2004a). Investigations of polypeptide rotational diffusion in aligned membranes by  $^2\text{H}$  and  $^{15}\text{N}$  solid-state NMR spectroscopy. *J. Am. Chem. Soc.* 126, 16676–16683.
- Aisenbrey, C., and Bechinger, B. (2004b). Tilt and rotational pitch angle of membrane-inserted polypeptides from combined  $^{15}\text{N}$  and  $^2\text{H}$  solid-state NMR spectroscopy. *Biochemistry* 43, 10502–10512.
- Antzutkin, O.N., and Tycko, R. (1999). High-order multiple quantum excitation in  $^{13}\text{C}$  nuclear magnetic resonance spectroscopy of organic solids. *J. Chem. Phys.* 110, 2749–2752.
- Antzutkin, O.N., Balbach, J.J., Leapman, R.D., Rizzo, N.W., Reed, J., and Tycko, R. (2000). Multiple quantum solid-state NMR indicates a parallel, not antiparallel, organization of  $\beta$ -sheets in Alzheimer's  $\beta$ -amyloid fibrils. *Proc. Natl. Acad. Sci. USA* 97, 13045–13050.
- Baldus, M. (2006). Solid-state NMR spectroscopy: molecular structure and organization at the atomic level. *Angew. Chem. Int. Ed. Engl.* 45, 1186–1188.
- Barre, P., Zschornig, O., Arnold, K., and Huster, D. (2003). Structural and dynamical changes of the bindin B18 peptide upon binding to lipid membranes. A solid-state NMR study. *Biochemistry* 42, 8377–8386.
- Bechinger, B., Aisenbrey, C., and Bertani, P. (2004). The alignment, structure and dynamics of membrane-associated polypeptides by solid-state NMR spectroscopy. *Biochim. Biophys. Acta* 1666, 190–204.
- Bockmann, A. (2006). Structural and dynamic studies of proteins by high-resolution solid-state NMR. *C. R. Chim.* 9, 381–392.
- Buffy, J.J., Hong, T., Yamaguchi, S., Waring, A., Lehrer, R.I., and Hong, M. (2003a). Solid-state NMR investigation of the depth of insertion of protegrin-1 in lipid bilayers using paramagnetic  $\text{Mn}^{2+}$ . *Biophys. J.* 85, 2363–2373.
- Buffy, J.J., Waring, A.J., Lehrer, R.I., and Hong, M. (2003b). Immobilization and aggregation of antimicrobial peptide protegrin in lipid bilayers investigated by solid-state NMR. *Biochemistry* 42, 13725–13734.
- Buffy, J.J., Waring, A.J., and Hong, M. (2005). Determination of peptide oligomerization in lipid membranes with magic-angle spinning spin diffusion NMR. *J. Am. Chem. Soc.* 127, 4477–4483.
- Cady, S.D., and Hong, M. (2006). Determining the orientation of rotationally diffusing membrane proteins using powder samples and magic-angle spinning: a  $^2\text{H}$ ,  $^{13}\text{C}$ , and  $^{15}\text{N}$  solid-state NMR investigation of a transmembrane helical bundle. In *Rocky Mountain Conference on Analytical Chemistry*: Breckenridge, CO.
- Chekmenov, E.Y., Hu, J., Gor'kov, P.L., Brey, W.W., Cross, T.A., Ruge, A., and Smirnov, A.I. (2005).  $^{15}\text{N}$  and  $^{31}\text{P}$  solid-state NMR study of transmembrane domain alignment of M2 protein of influenza A virus in hydrated cylindrical lipid bilayers confined to anodic aluminum oxide nanopores. *J. Magn. Reson.* 173, 322–327.
- De Angelis, A.A., Nevzorov, A.A., Park, S.H., Howell, S.C., Mrse, A.A., and Opella, S.J. (2004). High-resolution NMR spectroscopy of membrane proteins in aligned bicelles. *J. Am. Chem. Soc.* 126, 15340–15341.
- deAzevedo, E.R., Bonagamba, T.J., Hu, W., and Schmidt-Rohr, K. (1999). Centerband-only detection of exchange: efficient analysis of dynamics in solids by NMR. *J. Am. Chem. Soc.* 121, 8411–8412.

- deAzevedo, E.R., Bonagamba, T.J., Hu, W., and Schmidt-Rohr, K. (2000). Principle of centerband-only detection of the exchange and extension to a four-time CODEX. *J. Chem. Phys.* *112*, 8988–9001.
- Doherty, T., Waring, A.J., and Hong, M. (2006). Membrane-bound conformation and topology of the antimicrobial peptide tachyplesin-I by solid-state NMR. *Biochemistry*.
- Gaemers, S., and Bax, A. (2001). Morphology of three lyotropic liquid crystalline biological NMR media studied by translational diffusion anisotropy. *J. Am. Chem. Soc.* *123*, 12343–12352.
- Glaser, R.W., Grune, M., Wandelt, C., and Ulrich, A.S. (1999). Structure analysis of a fusogenic peptide sequence from the sea urchin fertilization protein bindin. *Biochemistry* *38*, 2560–2569.
- Glaser, R.W., Sachse, C., Durr, U.H., Wadhvani, P., and Ulrich, A.S. (2004). Orientation of the antimicrobial peptide PGLa in lipid membranes determined from 19F-NMR dipolar couplings of 4-CF3-phenylglycine labels. *J. Magn. Reson.* *168*, 153–163.
- Glaser, R.W., Sachse, C., Durr, U.H., Wadhvani, P., Afonin, S., Strandberg, E., and Ulrich, A.S. (2005). Concentration-dependent realignment of the antimicrobial peptide PGLa in lipid membranes observed by solid-state 19F-NMR. *Biophys. J.* *88*, 3392–3397.
- Grage, S.L., and Ulrich, A.S. (2000). Orientation-dependent (19F) dipolar couplings within a trifluoromethyl group are revealed by static multipulse NMR in the solid state. *J. Magn. Reson.* *146*, 81–88.
- Harroun, T.A., Koslowsky, M., Nieh, M.P., de Lannoy, C.F., Raghunathan, V.A., and Katsaras, J. (2005). Comprehensive examination of mesophases formed by DMPC and DHPC mixtures. *Langmuir* *21*, 5356–5361.
- Hiller, M., Krabben, L., Vinothkumar, K.R., Castellani, F., van Rossum, B.J., Kuhlbrandt, W., and Oschkinat, H. (2005). Solid-state magic-angle spinning NMR of outer-membrane protein G from *Escherichia coli*. *ChemBioChem* *6*, 1679–1684.
- Hong, M., and Doherty, T. (2006). Orientation determination of membrane-disruptive proteins using powder samples and rotational diffusion: a simple solid-state NMR approach. *Chem. Phys. Lett.* *432*, 296–300.
- Howard, K.P., Liu, W., Crocker, E., Nanda, V., Lear, J., Degrado, W.F., and Smith, S.O. (2005). Rotational orientation of monomers within a designed homo-oligomer transmembrane helical bundle. *Protein Sci.* *14*, 1019–1024.
- Huster, D. (2005). Investigations of the structure and dynamics of membrane-associated peptides by magic angle spinning NMR. *Prog. NMR Spectrosc.* *46*, 79–107.
- Huster, D., and Gawrisch, K. (1999). NOESY NMR crosspeaks between lipid headgroups and hydrocarbon chains: spin diffusion or molecular disorder? *J. Am. Chem. Soc.* *121*, 1992–1993.
- Huster, D., Arnold, K., and Gawrisch, K. (1999). Investigation of lipid organization in biological membranes by two-dimensional nuclear Overhauser enhancement spectroscopy. *J. Phys. Chem.* *103*, 243–251.
- Huster, D., Yao, X.L., and Hong, M. (2002). Membrane protein topology probed by 1H spin diffusion from lipids using solid-state NMR spectroscopy. *J. Am. Chem. Soc.* *124*, 874–883.
- Huster, D., Vogel, A., Katzka, C., Scheidt, H.A., Binder, H., Dante, S., Gutberlet, T., Zschornig, O., Waldmann, H., and Arnold, K. (2003). Membrane insertion of a lipidated ras peptide studied by FTIR, solid-state NMR, and neutron diffraction spectroscopy. *J. Am. Chem. Soc.* *125*, 4070–4079.
- Kamihira, M., Vosegaard, T., Mason, A.J., Straus, S.K., Nielsen, N.C., and Watts, A. (2005). Structural and orientational constraints of bacteriorhodopsin in purple membranes determined by oriented-sample solid-state NMR spectroscopy. *J. Struct. Biol.* *149*, 7–16.
- Ketchum, R.R., Hu, W., and Cross, T.A. (1993). High resolution conformation of Gramicidine A in a lipid bilayer by solid-state NMR. *Science* *261*, 1457–1460.
- Lange, A., Giller, K., Hornig, S., Martin-Eauclaire, M.F., Pongs, O., Becker, S., and Baldus, M. (2006). Toxin-induced conformational changes in a potassium channel revealed by solid-state NMR. *Nature* *440*, 959–962.
- Liu, W., Crocker, E., Siminovitich, D.J., and Smith, S.O. (2003). Role of side-chain conformational entropy in transmembrane helix dimerization of glycophorin A. *Biophys. J.* *84*, 1263–1271.
- Liu, W., Crocker, E., Constantinescu, S.N., and Smith, S.O. (2005). Helix packing and orientation in the transmembrane dimer of gp55-P of the spleen focus forming virus. *Biophys. J.* *89*, 1194–1202.
- Lorigan, G.A., Dave, P.C., Tiburu, E.K., Damodaran, K., Abu-Baker, S., Karp, E.S., Gibbons, W.J., and Minto, R.E. (2004). Solid-state NMR spectroscopic studies of an integral membrane protein inserted into aligned phospholipid bilayer nanotube arrays. *J. Am. Chem. Soc.* *126*, 9504–9505.
- Luca, S., White, J.F., Sohal, A.K., Filippov, D.V., van Boom, J.H., Grishammer, R., and Baldus, M. (2003). The conformation of neurotensin bound to its G protein-coupled receptor. *Proc. Natl. Acad. Sci. USA* *100*, 10706–10711.
- Ludtke, S.J., He, K., Heller, W.T., Harroun, T.A., Yang, L., and Huang, H.W. (1996). Membrane pores induced by magainin. *Biochemistry* *35*, 13723–13728.
- Mani, R., Cady, S.D., Tang, M., Waring, A.J., Lehrer, R.I., and Hong, M. (2006a). Membrane-dependent oligomeric structure and pore formation of a  $\beta$ -hairpin antimicrobial peptide in lipid bilayers from solid-state NMR. *Proc. Natl. Acad. Sci. USA* *103*, 16242–16247.
- Mani, R., Tang, M., Wu, X., Buffy, J.J., Waring, A.J., Sherman, M.A., and Hong, M. (2006b). Membrane-bound dimer structure of a  $\beta$ -hairpin antimicrobial peptide from rotational-echo double-resonance solid-state NMR. *Biochemistry* *45*, 8341–8349.
- Marassi, F.M., and Opella, S.J. (2003). Simultaneous assignment and structure determination of a membrane protein from NMR orientational restraints. *Protein Sci.* *12*, 403–411.
- Mascioni, A., and Veglia, G. (2003). Theoretical analysis of residual dipolar coupling patterns in regular secondary structures of proteins. *J. Am. Chem. Soc.* *125*, 12520–12526.
- McDermott, A.E. (2004). Structural and dynamic studies of proteins by solid-state NMR spectroscopy: rapid movement forward. *Curr. Opin. Struct. Biol.* *14*, 554–561.
- Mesleh, M.F., Lee, S., Veglia, G., Thiriou, D.S., Marassi, F.M., and Opella, S.J. (2003). Dipolar waves map the structure and topology of helices in membrane proteins. *J. Am. Chem. Soc.* *125*, 8928–8935.
- Opella, S.J., and Marassi, F.M. (2004). Structure determination of membrane proteins by NMR spectroscopy. *Chem. Rev.* *104*, 3587–3606.
- Opella, S.J., Marassi, F.M., Gesell, J.J., Valente, A.P., Kim, Y., Oblatt-Montal, M., and Montal, M. (1999). Structures of the M2 channel-lining segments from nicotinic acetylcholine and NMDA receptors by NMR spectroscopy. *Nat. Struct. Biol.* *6*, 374–379.
- Park, S.H., and Opella, S.J. (2005). Tilt angle of a trans-membrane helix is determined by hydrophobic mismatch. *J. Mol. Biol.* *350*, 310–318.
- Park, S.H., Mrse, A.A., Nevzorov, A.A., Mesleh, M.F., Oblatt-Montal, M., Montal, M., and Opella, S.J. (2003). Three-dimensional structure of the channel-forming trans-membrane domain of virus protein “u” (Vpu) from HIV-1. *J. Mol. Biol.* *333*, 409–424.
- Park, S.H., Mrse, A.A., Nevzorov, A.A., De Angelis, A.A., and Opella, S.J. (2006a). Rotational diffusion of membrane proteins in aligned phospholipid bilayers by solid-state NMR spectroscopy. *J. Magn. Reson.* *178*, 162–165.
- Park, S.H., Prytulla, S., De Angelis, A.A., Brown, J.M., Kiefer, H., and Opella, S.J. (2006b). High-resolution NMR spectroscopy of a GPCR in aligned bicelles. *J. Am. Chem. Soc.* *128*, 7402–7403.
- Prosser, R.S., Hwang, J.S., and Vold, R.R. (1998). Magnetically aligned phospholipid bilayers with positive ordering: a new model membrane system. *Biophys. J.* *74*, 2405–2418.
- Prosser, R.S., Luchette, P.A., and Westerman, P.W. (2000). Using O2 to probe membrane immersion depth by 19F NMR. *Proc. Natl. Acad. Sci. USA* *97*, 9967–9971.
- Prosser, R.S., Evanics, F., Kitevski, J.L., and Al-Abdul-Wahid, M.S. (2006). Current applications of bicelles in NMR studies of membrane-associated amphiphiles and proteins. *Biochemistry* *45*, 8453–8465.

- Saffman, P.G., and Delbruck, M. (1975). Brownian motion in biological membranes. *Proc. Natl. Acad. Sci. USA* **72**, 3111–3113.
- Salgado, J., Grage, S.L., Kondejewski, L.H., Hodges, R.S., McElhane, R.N., and Ulrich, A.S. (2001). Membrane-bound structure and alignment of the antimicrobial  $\beta$ -sheet peptide gramicidin S derived from angular and distance constraints by solid-state  $^{19}\text{F}$ -NMR. *J. Biomol. NMR* **21**, 191–208.
- Sanders, C.R., Hare, B.J., Howard, K.P., and Prestegard, J.H. (1994). Magnetically oriented phospholipid micelles as a tool for the study of membrane associated molecules. *Prog. NMR Spectrosc.* **26**, 421–444.
- Schmidt-Rohr, K., and Hong, M. (2003). Measurements of carbon to amide-proton distances by C-H dipolar recoupling with  $^{15}\text{N}$  NMR detection. *J. Am. Chem. Soc.* **125**, 5648–5649.
- Smith, S.O., Kawakami, T., Liu, W., Ziliox, M., and Aimoto, S. (2001a). Helical structure of phospholamban in membrane bilayers. *J. Mol. Biol.* **313**, 1139–1148.
- Smith, S.O., Song, D., Shekar, S., Groesbeek, M., Ziliox, M., and Aimoto, S. (2001b). Structure of the transmembrane dimer interface of glycophorin A in membrane bilayers. *Biochemistry* **40**, 6553–6558.
- Smith, S.O., Smith, C., Shekar, S., Peersen, O., Ziliox, M., and Aimoto, S. (2002). Transmembrane interactions in the activation of the Neu receptor tyrosine kinase. *Biochemistry* **41**, 9321–9332.
- Song, Z., Kovacs, F.A., Wang, J., Denny, J.K., Shekar, S.C., Quine, J.R., and Cross, T.A. (2000). Transmembrane domain of M2 protein from influenza A virus studied by solid-state  $^{15}\text{N}$  polarization inversion spin exchange at magic angle NMR. *Biophys. J.* **79**, 767–775.
- Strandberg, E., Tremouilhac, P., Wadhvani, P., and Ulrich, A.S. (2006). Realignment of membrane-bound antimicrobial peptides studied by solid-state  $^2\text{H}$ - and  $^{19}\text{F}$ -NMR. In *Rocky Mountain Conference on Analytical Chemistry: Breckenridge, CO*.
- Tian, F., Song, Z., and Cross, T.A. (1998). Orientational constraints derived from hydrated powder samples by two-dimensional PISEMA. *J. Magn. Reson.* **135**, 227–231.
- Toke, O., Maloy, W.L., Kim, S.J., Blazyk, J., and Schaefer, J. (2004a). Secondary structure and lipid contact of a peptide antibiotic in phospholipid bilayers by REDOR. *Biophys. J.* **87**, 662–674.
- Toke, O., O'Connor, R.D., Weldeghiorghis, T.K., Maloy, W.L., Glaser, R.W., Ulrich, A.S., and Schaefer, J. (2004b). Structure of (KIAGKIA) $_3$  aggregates in phospholipid bilayers by solid-state NMR. *Biophys. J.* **87**, 675–687.
- Tuzi, S., Hasegawa, J., Kawaminami, R., Naito, A., and Saito, H. (2001). Regio-selective detection of dynamic structure of transmembrane  $\alpha$ -helices as revealed from  $^{13}\text{C}$  NMR spectra of  $[\text{3-}^{13}\text{C}]\text{Ala}$ -labeled bacteriorhodopsin in the presence of  $\text{Mn}^{2+}$  ion. *Biophys. J.* **81**, 425–434.
- Ulrich, A.S., Otter, M., Glabe, C.G., and Hoekstra, D. (1998). Membrane fusion is induced by a distinct peptide sequence of the sea urchin fertilization protein bindin. *J. Biol. Chem.* **273**, 16748–16755.
- van Dam, L., Karlsson, G., and Edwards, K. (2004). Direct observation and characterization of DMPC/DHPC aggregates under conditions relevant for biological solution NMR. *Biochim. Biophys. Acta* **1664**, 241–256.
- van Dam, L., Karlsson, G., and Edwards, K. (2006). Morphology of magnetically aligning DMPC/DHPC aggregates-perforated sheets, not disks. *Langmuir* **22**, 3280–3285.
- Vogel, A., Katzka, C.P., Waldmann, H., Arnold, K., Brown, M.F., and Huster, D. (2005). Lipid modifications of a Ras peptide exhibit altered packing and mobility versus host membrane as detected by  $^2\text{H}$  solid-state NMR. *J. Am. Chem. Soc.* **127**, 12263–12272.
- Wang, J., Kim, S., Kovacs, F., and Cross, T.A. (2001). Structure of the the transmembrane region of the M2 protein  $\text{H}^+$  channel. *Protein Sci.* **10**, 2241–2250.
- Yamaguchi, S., Huster, D., Waring, A., Lehrer, R.I., Tack, B.F., Kearney, W., and Hong, M. (2001). Orientation and dynamics of an antimicrobial peptide in the lipid bilayer by solid-state NMR. *Biophys. J.* **81**, 2203–2214.
- Yamaguchi, S., Waring, A., Hong, T., Lehrer, R., and Hong, M. (2002). Solid-State NMR investigations of peptide-lipid interaction and orientation of a  $\beta$ -sheet antimicrobial peptide, protegrin. *Biochemistry* **41**, 9852–9862.
- Yang, J., and Weliky, D.P. (2003). Solid-state nuclear magnetic resonance evidence for parallel and antiparallel strand arrangements in the membrane-associated HIV-1 fusion peptide. *Biochemistry* **42**, 11879–11890.
- Yang, J., Gabrys, C.M., and Weliky, D.P. (2001). Solid-state nuclear magnetic resonance evidence for an extended  $\beta$  strand conformation of the membrane-bound HIV-1 fusion peptide. *Biochemistry* **40**, 8126–8137.
- Yang, J., Prorok, M., Castellino, F.J., and Weliky, D.P. (2004). Oligomeric  $\beta$ -structure of the membrane-bound HIV-1 fusion peptide formed from soluble monomers. *Biophys. J.* **87**, 1951–1963.
- Yen, Y., and Pines, A. (1983). Multiple-quantum NMR in solids. *J. Chem. Phys.* **78**, 3579–3582.